



HAL
open science

Keratinocyte-specific ablation of the NF- κ B regulatory protein A20 (TNFAIP3) reveals a role in the control of epidermal homeostasis

Wim Declercq, Saskia Lippens, Sylvie Lefebvre, Barbara Gilbert, Mozes Sze, Michael Devos, Lars Vereecke, Conor Mcguire, Christopher J. Guerin, Peter Vandenabeele, et al.

► **To cite this version:**

Wim Declercq, Saskia Lippens, Sylvie Lefebvre, Barbara Gilbert, Mozes Sze, et al.. Keratinocyte-specific ablation of the NF- κ B regulatory protein A20 (TNFAIP3) reveals a role in the control of epidermal homeostasis. *Cell Death and Differentiation*, 2011, 10.1038/cdd.2011.55 . hal-00640518

HAL Id: hal-00640518

<https://hal.science/hal-00640518>

Submitted on 13 Nov 2011

HAL is a multi-disciplinary open access archive for the deposit and dissemination of scientific research documents, whether they are published or not. The documents may come from teaching and research institutions in France or abroad, or from public or private research centers.

L'archive ouverte pluridisciplinaire **HAL**, est destinée au dépôt et à la diffusion de documents scientifiques de niveau recherche, publiés ou non, émanant des établissements d'enseignement et de recherche français ou étrangers, des laboratoires publics ou privés.

Keratinocyte-specific ablation of the NF- κ B regulatory protein A20 (TNFAIP3) reveals a role in the control of epidermal homeostasis

Saskia Lippens^{1,2}, Sylvie Lefebvre³, Barbara Gilbert^{1,2}, Mozes Sze^{1,2}, Michael Devos^{1,2}, Kelly Verhelst^{1,2}, Lars Vereecke^{1,2}, Conor Mc Guire^{1,2}, Chris Guérin^{1,2}, Peter Vandenabeele^{1,2}, Manolis Pasparakis⁴, Marja L. Mikkola³, Rudi Beyaert^{1,2*}, Wim Declercq^{1,2*} and Geert van Loo^{1,2*}

¹*Department for Molecular Biomedical Research, VIB, B-9052 Ghent, Belgium.*

²*Department of Biomedical Molecular Biology, Ghent University, B-9052 Ghent, Belgium.*

³*Developmental Biology Program, Institute of Biotechnology, University of Helsinki, F-00014 Helsinki, Finland.*

⁴*Institute for Genetics, University of Cologne, D-50674 Cologne, Germany.*

*These authors share senior authorship

Address correspondence to: geert.vanloo@dibr.vib-UGent.be or wim.declercq@dibr.vib-UGent.be or rudi.beyaert@dibr.vib-UGent.be

Running title: A20 controls skin homeostasis

Summary

The ubiquitin-editing enzyme A20 (TNFAIP3) serves as a critical brake on NF- κ B signaling. In humans, polymorphisms in or near the *A20* gene are associated with several inflammatory disorders, including psoriasis. We show here that epidermis-specific A20 knockout mice ($A20^{EKO}$) develop keratinocyte hyperproliferation, but no signs of skin inflammation, such as immune cell infiltration. However, $A20^{EKO}$ mice clearly developed ectodermal organ abnormalities, including disheveled hair, longer nails and sebocyte hyperplasia. This phenotype resembles that of mice overexpressing EDA-A1 or its receptor EDAR, suggesting that A20 negatively controls EDAR signaling. We found that A20 inhibited EDAR-induced NF- κ B signaling independent from its de-ubiquitinating activity. In addition, A20 expression was induced by EDA-A1 in embryonic skin explants, where its expression was confined to the hair placodes, known to be the site of EDAR expression. In summary, our data indicate that EDAR-induced NF- κ B levels are controlled by A20, which acts as a negative feedback regulator, to assure proper skin homeostasis and epidermal appendage development.

Introduction

The epidermis consists mainly of keratinocytes organized in different layers. The basal layer keratinocytes are mitotically active and provide new cells that gradually undergo differentiation towards the skin surface, where they cornify and are shed.¹ This well orchestrated biological process is tightly controlled, and distortions in the sequence of events can result in different skin disorders, including inflammation and cancer. An exact control of the transcription factor NF- κ B is essential to maintain skin homeostasis, witnessed by the fact that NF- κ B overactivity as well as the ablation of essential NF- κ B activators lead to skin inflammation.²⁻⁴ NF- κ B belongs to a family of structurally related and evolutionarily conserved proteins (p100 or NF- κ B2, p105 or NF- κ B1, p65 or RelA, RelB, c-Rel), which exist as homo- or heterodimers. In resting cells, NF- κ B is kept inactive by binding to inhibitor of κ B (I κ B) proteins, of which I κ B α is the most studied. Numerous stimuli lead to phosphorylation and polyubiquitination of I κ B proteins, which targets them for proteasomal degradation. This results in the release of NF- κ B, which accumulates in the nucleus and transcriptionally activates target genes.⁵

A central event in NF- κ B signaling is the activation of the I κ B kinase (IKK) complex, which consists of two kinases, IKK1 and IKK2 (also known as IKK α and IKK β), and a regulatory platform protein, NEMO (NF- κ B essential modulator, also known as IKK γ). Gene targeting experiments showed that IKK2 and NEMO, but not IKK1, are required for NF- κ B activation by TNF and by Toll-like receptors (TLRs).⁴ Some receptors, such as those for lymphotoxin β and CD40, can activate an alternative NF- κ B pathway involving IKK1 and

leading to processing of p100 NF- κ B to p52, which forms a transcriptionally active dimer with RelB.

As shown by skin-specific ablation of different NF- κ B activators, cell autonomous activity of NF- κ B seems to prevent keratinocyte apoptosis in both homeostatic and TNF-dependent inflammatory conditions.^{2, 6-10} As expected, overactivation of NF- κ B in keratinocytes results in skin inflammation.¹¹⁻¹³ Besides its role in controlling inflammation and preventing apoptosis, NF- κ B is also involved in the development of epidermal derivatives, such as hair, nails and sweat glands,^{14, 15} in which signaling is initiated by the binding of EDA-A1 to the epidermal-specific TNF-R family member EDAR.^{16,17} EDAR acts through EDARADD, TRAF6 and TAB2/TAK1 to activate the IKK complex.^{18, 19} Human mutations in the *Eda1*, *Edar*, or *Edaradd* genes result in hypohydrotic ectodermal dysplasia (HED) characterized by defects in development of hair, teeth and sweat glands.²⁰⁻²⁴ Similarly, mice carrying mutations in these genes, or lacking them or *Traf6*, acquire HED.^{18, 25-30} Transgenic mice overexpressing EDA-A1 or EDAR develop morphogenetic alterations in a variety of ectodermal organs, including hair and teeth, and sweat, mammary and sebaceous glands,³¹⁻³⁶ which indicates that overactivation of the EDA/EDAR pathway is detrimental for development of epidermal appendages.

As NF- κ B is crucial in development and inflammation, tight regulation of its activation is essential. This tight control is achieved by the combined action of positive and negative regulators.³⁷ During recent years, ubiquitination and de-ubiquitination of several NF- κ B signaling components have been identified as crucial steps in the control of NF- κ B signaling pathways.³⁸ One critical brake on NF- κ B activation is the ubiquitin-editing

enzyme A20, which has been characterized as an inhibitor of both NF- κ B activation and apoptosis.³⁹ A20 is required for terminating NF- κ B signaling in response to TNF⁴⁰ and microbial products such as lipopolysaccharide (LPS) and muramyl dipeptide (MDP).^{41, 42} The *in vivo* importance of the A20 anti-inflammatory activities is illustrated by severe multi-organ inflammation and perinatal death seen in A20^{-/-} mice.⁴⁰ Recent genetic studies demonstrate an association between the human *A20/TNFAIP3* gene and autoimmune pathology and psoriasis, which suggests that A20 might play an important role in human autoimmune and inflammatory diseases.⁴³ These findings emphasize the importance of A20 in the control of normal tissue homeostasis and identify it as a potential target for treatment of multiple inflammatory pathologies, including psoriasis.

We used K14-driven Cre/LoxP-mediated gene targeting in mice to investigate the *in vivo* function of A20 in epidermal development and homeostasis. We show that A20 is essential for controlling keratinocyte proliferation and for proper development of ectodermal appendages. Our data indicate that keratinocyte-specific deletion of A20 results in excessive EDA-A1-induced NF- κ B signaling, thereby phenocopying EDA-A1 transgenic mice.

Results

Generation of epidermis-specific A20-deficient mice

To identify the tissue-specific functions of A20, we generated mice carrying a conditional A20 allele in which exons IV and V of the mouse A20 gene are flanked by LoxP-sites⁴⁴. To study the function of A20 in skin and epidermal appendages, we crossed the A20^{FL/FL} mice with a transgenic mouse line that expresses Cre under the control of the human *Keratin14* gene promoter (K14-Cre).⁴⁵ Epidermal keratinocyte-specific A20 knockout mice (A20^{FL/FL}/K14-Cre, A20^{EKO}) were born with normal Mendelian segregation (data not shown). To verify keratinocyte-specific A20 deletion in A20^{EKO} mice (Fig. 1A), we confirmed by southern blot analysis that there was efficient Cre-mediated recombination in epidermis and in primary keratinocytes (Fig. 1B). Consequently, we could not detect endogenous A20 in epidermal extracts from A20^{EKO} mice (Fig. 1C).

A20^{EKO} mice show keratinocyte hyperplasia

Macroscopic signs of skin inflammation, such as redness, scaling or excessive scratching due to itch, were not observed in A20^{EKO} mice (Fig. 1A). Histological analysis of back skin sections showed a thickened epidermis due to increased proliferation (2.5-fold) of the basal cells (Fig. 2A, 2B and 2C), but similar very low levels of apoptosis (data not shown). The expression patterns of the differentiation markers caspase-14, filaggrin and keratin 10 were normal, and infiltrating immune cells were not observed (data not shown). These data indicate that absence of A20 does not lead to spontaneous skin

inflammation, or that other de-ubiquitinating enzymes, such as CYLD⁴⁶, act redundantly to prevent spontaneous inflammation.

A20^{EKO} mice display abnormalities in ectodermal appendages

The coat of A20^{EKO} mice was disorganized (Fig. 1A and 3A). This disheveled hair phenotype was never observed in A20^{FL/FL} control littermates. Mice were monitored up to the age of 12 months and did not exhibit signs of hair loss or alopecia. A20^{FL/FL} mice were also crossed to a K5-Cre transgenic line,⁴⁷ with which a similar phenotype was observed (data not shown). All further experiments were done on A20^{FL/FL}/K14-Cre mice.⁴⁵

Four hair types can be distinguished in the mouse coat. Awl and guard hairs are straight, whereas auchene and zigzag hairs have one or multiple bends, respectively. Although straight hairs were found in A20^{EKO} mice, other hair types had a curly instead of a bended morphology (Fig. 3B). Upon epilating A20^{EKO} mice, we noticed that the hair was more fragile and thinner than the hair of A20^{FL/FL} mice. The increased fragility of A20^{EKO} hair was further confirmed by testing its resistance to sonication (data not shown). Scanning electron microscopy (SEM) analysis confirmed extensive cuticle damage in hair fibers of A20^{EKO} mice (Fig. 3C and 3D). This hair damage can be explained by the amorphous nature of the hair cuticle, which, as observed by transmission electron microscopy, lacked a clear structure (Fig. 3E and 3F). The medulla of the A20^{EKO} hair is similar to that of wild type mice (data not shown). The A20^{EKO} hair phenotype is strikingly similar to that of mice with keratinocyte-specific transgenes for EDA-A1 or EDAR.^{31-33, 48, 49} The EDA-A1-induced NF-κB pathway is required for development of epidermal

appendages, including hair, and its hyperactivity results in disheveled hair, longer nail growth, sebocyte hyperplasia, and the induction of additional molar-like teeth and nipples in mice.³¹⁻³⁶ A20^{EKO} mice also display longer nails (Fig. 4A), larger scale-like folds and more curly hair on the tails (Fig. 4B), and sebocyte hyperplasia (Fig. 4C and 4D). Extra teeth or nipples were never observed in A20^{EKO} mice.

A20 acts as a regulator of the Ectodysplasin pathway to NF-κB activation

Because loss of A20 in the skin results in partial phenocopy of EDA-A1 overexpression in keratinocytes, we hypothesized that A20 might be a negative regulator of the Ectodysplasin pathway. Indeed, by using an NF-κB-dependent luciferase reporter assay we demonstrated that A20 blocks EDAR-induced activation of NF-κB in HEK293T cells to a similar extent as TNF-induced NF-κB activation (Fig. 5A). Making use of deletion mutants, we could demonstrate that EDAR-induced NF-κB activation was inhibited by the C-terminal domain of A20, containing the Zn-fingers, but not by the N-terminal de-ubiquitinating (DUB) domain (Fig. 5B and Suppl. Fig. 1), suggesting that the DUB activity is not required for inhibition of NF-κB activation. To verify this, we also tested a double point mutant (A20 D100A/C103A), which has no DUB activity⁵⁰ (Fig. 5C and Suppl. Fig. 1). A20 D100A/C103A was as effective as wild type A20 in inhibiting EDAR-induced NF-κB, confirming that the A20 DUB activity is not required for this effect.

In addition, both A20 mRNA and protein levels were increased after EDA-A1 treatment of embryonic skin explants of *Eda* deficient mice (*Tabby*; hereafter *Eda*^{-/-}, Fig. 5D and 5E). This indicates that A20 is an NF-κB response gene in

the Ectodysplasin pathway acting in negative feedback regulation of EDAR-induced NF- κ B signaling. Interestingly, the expression pattern of A20 in the skin of developing embryos (E 14) appears to be limited to the hair placode (Fig. 6A), i.e. at sites of EDAR expression and NF- κ B activity.^{14, 51} This indicates that under homeostatic conditions, A20 functions mainly in the hair follicle to prevent overactivation of EDAR. We could not detect A20 in mammary buds or tooth placodes of E12 embryos (Fig. 6B). However, it was previously reported that A20 is expressed at later stages of tooth development, as well as in secondary hair follicles and vibrissae.⁵² In conclusion, these data indicate that the phenotype of the A20^{EKO} mice is due to overactivity of the Ectodysplasin pathway in the absence of A20.

Discussion

Like I κ B α , A20 is an important negative regulator of NF- κ B signaling and inflammation.⁴³ However, their modes of action are totally different. I κ B α acts by binding NF- κ B directly and sequestering it away from the nucleus,⁵³ whereas A20 is a ubiquitin-editing enzyme that inactivates multiple targets in the NF- κ B pathway.⁴³ I κ B α is always present in unstimulated cells to restrain uncontrolled NF- κ B activation in the absence of a specific inflammatory trigger. In contrast, in most unstimulated cells, expression of A20 is weak, but it is strongly induced once NF- κ B signaling is switched on.³⁹ Because also I κ B α expression is further induced upon NF- κ B triggering, both I κ B α and A20 are involved in a negative feedback loop of NF- κ B activation. The hyperinflammation in I κ B α or full A20 null mice, and their early death, point to critical functions of I κ B α and A20 in NF- κ B regulation.^{13, 40, 54, 55}

Excessive NF- κ B signaling in the skin, such as in keratinocyte-specific I κ B α knockout mice and K5-IKK2 transgenic mice, induces skin inflammation.^{12, 13} Unexpectedly, though A20^{EKO} mice developed epidermal hyperproliferation, they did not develop spontaneous inflammation. The presence of a functional I κ B α might be sufficient to control minor inflammatory responses against environmental insults. Alternatively, redundant de-ubiquitinating enzymes that control NF- κ B activation, such as CYLD (cylindromatosis), might be active in the skin. Although CYLD is prominently expressed in the epidermis, CYLD^{-/-} mice do not exhibit skin abnormalities⁴⁶. It is possible that ablation of both A20 and CYLD is required for spontaneous severe skin inflammation.

We show that epidermis-specific A20 deletion leads to multiple abnormalities in ectodermal organs, similar to overactivation of the Ectodysplasin

pathway.^{32-36, 56} The resemblance of A20^{EKO} mice to mice overexpressing EDA-A1/EDAR and the inhibition of EDAR signaling by A20 *in vitro* strongly suggest that hyperactivation of the Ectodysplasin pathway is the primary cause of the A20^{EKO} phenotype. This conclusion is further supported by our finding that EDA-A1 induces A20 expression and that A20 mRNA co-localizes with *Edar* and NF- κ B signaling activity in developing hair follicles. A20 is known to inhibit NF- κ B signaling induced by different signaling pathways and was shown to depend on the DUB activity of its OTU domain and the ubiquitin ligating activity of the C-terminal Zn-fingers.^{57, 58} We could demonstrate that the DUB activity of A20 is not involved in inhibition of EDAR signaling.

Similarities between A20^{EKO} mice and EDA-A1 transgenic mice include nail and hair defects, and sebaceous gland hyperplasia. EDA-A1 transgenics also develop extra teeth and nipples,³² but these abnormalities were never observed in A20^{EKO} mice. It is possible that EDA-A1 signaling is not regulated by A20 at these sites, which correlates with the lack of detectable A20 expression in tooth placodes and mammary buds. It is also possible that formation of supernumerary tooth and mammary buds requires more potent EDAR activity, which can be achieved by excessive ligand production but not by removal of a negative feedback mechanism that attenuates signaling. Another explanation is that K14-Cre-mediated deletion of A20 may have taken place too late to allow induction of ectopic organ primordia, because K14-Cre expression is strongest at E15, whereas induction of tooth and mammary placodes starts at E11 to E12.⁵⁹

In conclusion, we identified A20 as an EDA-A1-induced protein acting as an inhibitor of EDAR-dependent NF- κ B signaling, independent from its DUB activity. As a consequence, genetic deletion of A20 in keratinocytes affects normal epidermal appendage development, similar as observed in transgenic mice overexpressing EDA-A1 or EDAR.

Experimental Procedures

A20^{EKO}, Eda^{-/-} and K14-EDA mice

Mice with a conditional A20 allele, in which exons IV and V of A20 are flanked with two LoxP sites, were generated as described.⁴⁴ All experiments were performed on mice backcrossed into the C57BL/6 background for at least five generations. Mice were housed in individually ventilated cages at the VIB Department for Molecular Biomedical Research in a specific pathogen-free animal facility. EDA-deficient mice were purchased from the Jackson Laboratories (*Tabby*, stock #JR0314). All experiments on mice were conducted according to institutional, national, and European animal regulations and were approved by the local Ethics Committee.

Southern blotting

Ten micrograms of genomic DNA was digested with *Bam*HI to differentiate between the 6.5-kb and 13.5-kb fragments of A20^{FL} and A20^{EKO} alleles, respectively. DNA was separated in agarose gels and transferred to nitrocellulose. DNA was hybridized with a ³²P-labeled probe.

Hair analysis

Hairs from A20^{FL/FL} and A20^{EKO} mice were obtained from the back and examined with a stereomicroscope.

NF- κ B luciferase reporter assay

Human A20 truncation mutants A20-N (AA 1-376) and A20-C (AA 377-790), and A20 D100A/C103A double-mutant, with aminoterminal E-tag were cloned in the pCAGGS expression plasmid. HEK293T cells were transfected with the indicated expression vectors combined with 100 ng of reporter plasmids for NF- κ B-luciferase and pACT- β -galactosidase. After 24 h, the cells were collected, washed in PBS and lysed in Luciferase lysis buffer (25 mM Tris phosphate pH 7.8, 2 mM DTT, 2 mM CDTA, 10% glycerol and 1% Triton-X-100). Substrate buffer was added (658 mM luciferin, 378 mM coenzyme A and 742 mM ATP) and Luciferase activity (Luc) was assayed in a GloMax 96 Microplate Luminometer (Promega). B-Galactosidase (Gal) activity in cell extracts was assayed with chlorophenol red β -D-galactopyranoside substrate (Roche Applied Science, Basel, Switzerland) and the optical density was read at 595 nm in a Benchmark microplate Reader (Bio-Rad Laboratories, Nazareth, Belgium). Luc values were normalized for Gal values to correct for differences in transfection efficiency (plotted as Luc/Gal). The data represent the average \pm S.D. of triplicates.

Histological and immunohistochemical analysis

Tissues were fixed for 2 h in 4% paraformaldehyde and embedded in paraffin. Sections of 5 μ m were processed for immunohistochemical analysis, and anti-Ki-67 (Dako EnVision System, Glostrup, Denmark) or anti-adipophilin was

used as primary antibody (Fitzgerald Industries Int., Acton, MA, USA). The primary antibody was detected with the appropriate HRP (DAB) kit (Dako EnVision System, Glostrup, Denmark). The number of Ki-67-positive and -negative cells in the basal layer was counted. The percentage of Ki-67 positive cells was determined and results are expressed as the mean \pm S.D. The surface area of the sebaceous gland was measured with Volocity software, based on adipophilin staining. The total number of sebaceous glands measured was 139 in four A20^{FL/FL} mice and 319 in five A20^{EKO} mice. Mean surface area \pm SEM is shown. Statistical significance between experimental groups was assessed using an unpaired two-sample Student t-Test. *p* values less than 0.05 were considered to indicate statistical significance.

Transmission electron microscopy

Mice were anesthetized and then euthanized by perfusion fixation through the vascular system with 4% paraformaldehyde. After washing, skin samples were postfixed in 1% OsO₄ with K₃Fe(CN)₆ in 0.1 M NaCacodylate buffer, pH 7.2. Samples were dehydrated through a graded ethanol series, including en-bloc staining with 2% uranyl acetate at the 50% ethanol step, and then embedded in Spurr's resin. Ultrathin sections of approximately 150 nm were cut using an ultramicrotome (Leica EM UC6, Leica Microsystems, Mannheim, Germany), and collected on formvar-coated copper grids. They were post-stained with uranyl acetate and lead citrate in a Leica EM AC20 autostainer and viewed with a JEOL 1010 transmission electron microscope (JEOL,

Tokyo, Japan) at 80 kV and digital images were captured on reusable image plates.

Scanning electron microscopy

Samples of hair for SEM were mounted on specimen stubs with double-sided tape and coated with gold using a Polaron SC 7620 Sputter coater (Quorum Technologies, East Sussex, UK). Samples were viewed with a Hitachi TM-1000 scanning electron microscope (Hitachi High-Technologies GmbH, Krefeld, Germany) and images were captured directly as digital files.

Skin explant culture and quantitative RT-PCR

Embryonic skin explants were cultured as previously described.^{60, 61} In brief, E14 EDA^{-/-} back skins were dissected, cut into halves along the midline, and cultured for 2 (10 samples) or 4 hours (9 samples) in a 30- μ l hanging drop of DMEM, 10% FCS, glutamine, and penicillin-streptomycin. One half was supplemented with 250 ng/ml of recombinant Fc-Eda-A1 protein,⁶² and the control half with PBS, 0.1% BSA. For RNA isolation, skin explants were harvested in 350 μ l of Rneasy (Qiagen) lysis buffer as specified by the manufacturer. 300 ng of Dnase-treated RNA was reverse transcribed with Superscript II (Invitrogen), and quantitative PCR was performed in a LightCycler480 (Roche). Transcript number was quantified by comparison with PCR product dilutions of the genes of interest using Lightcycler480 software provided by the manufacturer. Expression of each gene was normalized against *Ranbp1*. The primer sequences were as follows: A20 forward: 5'AGGCTATGACAGCCAGCACT3'; A20 reverse

5'AAACCTACCCCGGTCTCTGT3'. Statistical significance between experimental groups was assessed using a paired Student t-Test.

In situ hybridization

Embryos were fixed overnight in 4% paraformaldehyde and dehydrated in a methanol series. Whole mount *in situ* hybridization was carried out by the InSituPro robots (Intavis AG, Germany) as described earlier.⁶⁰ The following digoxigenin-labeled probes were used: a 656-bp probe specific for *A20* (nt 3223-3879 of NM_009397). A sense probe, used as a negative control, showed no positive signal in any of the hybridizations (data not shown). Some samples were embedded in 0.5% gelatin, 30% albumin, 20% sucrose and 2% glutaraldehyde in PBS and sectioned at 30 μ m using a vibratome.

Western blotting

Mouse epidermis was separated from dermis after 15 minutes of incubation in 3,8% ammonium thiocyanate. Epidermal extracts were prepared using lysis buffer containing 5 mM Hepes, 0,1% NP-40, 10% Glycerol, 150 mM NaCl, 5 mM EDTA. Skin explant lysates were prepared as follows: after 6h incubation in the hanging drop, epithelia were separated from the mesenchyme and homogenized in 2% SDS in PBS by boiling, and by using a syringe and needle. Protein concentration was determined using the BCATM Protein Assay kit (Pierce) according to the manufacturer instructions. 20 μ g of protein was separated in 10% SDS-PAGE, transferred onto a Hybond-C-extra membrane (Amersham), and probed with an anti-A20 antibody (Santa Cruz, sc-166692; 1:150) followed by HRP-conjugated anti-mouse secondary antibody (Jackson

Laboratories, 1:6 000). Blots were developed using enhanced chemiluminescence (SuperSignal West Pico, Thermo Scientific).

References

1. Blanpain C, Fuchs E. Epidermal homeostasis: a balancing act of stem cells in the skin. *Nat Rev Mol Cell Biol* 2009 Mar; **10** (3): 207-217.
2. Seitz CS, Freiberg RA, Hinata K, Khavari PA. NF-kappaB determines localization and features of cell death in epidermis. *J Clin Invest* 2000 Feb; **105** (3): 253-260.
3. Lippens S, Hoste E, Vandenabeele P, Agostinis P, Declercq W. Cell death in the skin. *Apoptosis* 2009 Apr; **14** (4): 549-569.
4. Pasparakis M, Luedde T, Schmidt-Supprian M. Dissection of the NF-kappaB signalling cascade in transgenic and knockout mice. *Cell Death Differ* 2006 May; **13** (5): 861-872.
5. Hayden MS, Ghosh S. Shared principles in NF-kappaB signaling. *Cell* 2008 Feb 8; **132** (3): 344-362.
6. Makris C, Godfrey VL, Krahn-Senftleben G, Takahashi T, Roberts JL, Schwarz T, *et al.* Female mice heterozygous for IKK gamma/NEMO deficiencies develop a dermatopathy similar to the human X-linked disorder incontinentia pigmenti. *Mol Cell* 2000 Jun; **5** (6): 969-979.
7. Schmidt-Supprian M, Bloch W, Courtois G, Addicks K, Israel A, Rajewsky K, *et al.* NEMO/IKK gamma-deficient mice model incontinentia pigmenti. *Mol Cell* 2000 Jun; **5** (6): 981-992.

8. Gugasyan R, Voss A, Varigos G, Thomas T, Grumont RJ, Kaur P, *et al.*
The transcription factors c-rel and RelA control epidermal development and homeostasis in embryonic and adult skin via distinct mechanisms. *Mol Cell Biol* 2004 Jul; **24** (13): 5733-5745.
9. Omori E, Matsumoto K, Sanjo H, Sato S, Akira S, Smart RC, *et al.*
TAK1 is a master regulator of epidermal homeostasis involving skin inflammation and apoptosis. *J Biol Chem* 2006 Jul 14; **281** (28): 19610-19617.
10. Sayama K, Hanakawa Y, Nagai H, Shirakata Y, Dai X, Hirakawa S, *et al.*
Transforming growth factor-beta-activated kinase 1 is essential for differentiation and the prevention of apoptosis in epidermis. *J Biol Chem* 2006 Aug 4; **281** (31): 22013-22020.
11. Dong J, Jimi E, Zeiss C, Hayden M, Ghosh S. Constitutively active NF-kappaB triggers systemic TNFalpha-dependent inflammation and localized TNFalpha-independent inflammatory disease. *Genes Dev* 2010; **24**: 1709-1717.
12. Page A, Navarro M, Garin M, Perez P, Casanova ML, Moreno R, *et al.*
IKKbeta leads to an inflammatory skin disease resembling interface dermatitis. *J Invest Dermatol* 2010 Jun; **130** (6): 1598-1610.
13. Rebholz B, Haase I, Eckelt B, Paxian S, Flaig MJ, Ghoreschi K, *et al.*
Crosstalk between keratinocytes and adaptive immune cells in an IkappaBalpha protein-mediated inflammatory disease of the skin. *Immunity* 2007 Aug; **27** (2): 296-307.

14. Pispá J, Pummila M, Barker PA, Thesleff I, Mikkola ML. Edar and Troy signalling pathways act redundantly to regulate initiation of hair follicle development. *Hum Mol Genet* 2008 Nov 1; **17** (21): 3380-3391.
15. Schmidt-Ullrich R, Aebischer T, Hulsken J, Birchmeier W, Klemm U, Scheidereit C. Requirement of NF-kappaB/Rel for the development of hair follicles and other epidermal appendices. *Development* 2001 Oct; **128** (19): 3843-3853.
16. Mikkola ML. TNF superfamily in skin appendage development. *Cytokine Growth Factor Rev* 2008 Jun-Aug; **19** (3-4): 219-230.
17. Yan M, Wang LC, Hymowitz SG, Schilbach S, Lee J, Goddard A, *et al.* Two-amino acid molecular switch in an epithelial morphogen that regulates binding to two distinct receptors. *Science* 2000 Oct 20; **290** (5491): 523-527.
18. Naito A, Yoshida H, Nishioka E, Satoh M, Azuma S, Yamamoto T, *et al.* TRAF6-deficient mice display hypohidrotic ectodermal dysplasia. *Proc Natl Acad Sci U S A* 2002 Jun 25; **99** (13): 8766-8771.
19. Morlon A, Munnich A, Smahi A. TAB2, TRAF6 and TAK1 are involved in NF-kappaB activation induced by the TNF-receptor, Edar and its adaptor Edaradd. *Hum Mol Genet* 2005 Dec 1; **14** (23): 3751-3757.
20. Bal E, Baala L, Cluzeau C, El Kerch F, Ouldin K, Hadj-Rabia S, *et al.* Autosomal dominant anhidrotic ectodermal dysplasias at the EDARADD locus. *Hum Mutat* 2007 Jul; **28** (7): 703-709.
21. Chassaing N, Bourthoumieu S, Cossee M, Calvas P, Vincent MC. Mutations in EDAR account for one-quarter of non-ED1-related

- hypohidrotic ectodermal dysplasia. *Hum Mutat* 2006 Mar; **27** (3): 255-259.
22. Kere J, Srivastava AK, Montonen O, Zonana J, Thomas N, Ferguson B, *et al.* X-linked anhidrotic (hypohidrotic) ectodermal dysplasia is caused by mutation in a novel transmembrane protein. *Nat Genet* 1996 Aug; **13** (4): 409-416.
23. Monreal AW, Zonana J, Ferguson B. Identification of a new splice form of the EDA1 gene permits detection of nearly all X-linked hypohidrotic ectodermal dysplasia mutations. *Am J Hum Genet* 1998 Aug; **63** (2): 380-389.
24. Smahi A, Courtois G, Rabia SH, Doffinger R, Bodemer C, Munnich A, *et al.* The NF-kappaB signalling pathway in human diseases: from incontinentia pigmenti to ectodermal dysplasias and immune-deficiency syndromes. *Hum Mol Genet* 2002 Oct 1; **11** (20): 2371-2375.
25. Headon DJ, Emmal SA, Ferguson BM, Tucker AS, Justice MJ, Sharpe PT, *et al.* Gene defect in ectodermal dysplasia implicates a death domain adapter in development. *Nature* 2001 Dec 20-27; **414** (6866): 913-916.
26. Mikkola ML, Thesleff I. Ectodysplasin signaling in development. *Cytokine Growth Factor Rev* 2003 Jun-Aug; **14** (3-4): 211-224.
27. Monreal AW, Ferguson BM, Headon DJ, Street SL, Overbeek PA, Zonana J. Mutations in the human homologue of mouse dl cause autosomal recessive and dominant hypohidrotic ectodermal dysplasia. *Nat Genet* 1999 Aug; **22** (4): 366-369.

28. Srivastava AK, Pispá J, Hartung AJ, Du Y, Ezer S, Jenks T, *et al.* The Tabby phenotype is caused by mutation in a mouse homologue of the EDA gene that reveals novel mouse and human exons and encodes a protein (ectodysplasin-A) with collagenous domains. *Proc Natl Acad Sci U S A* 1997 Nov 25; **94** (24): 13069-13074.
29. Thesleff I, Mikkola ML. Death receptor signaling giving life to ectodermal organs. *Sci STKE* 2002 May 7; **2002** (131): pe22.
30. Yan M, Zhang Z, Brady JR, Schilbach S, Fairbrother WJ, Dixit VM. Identification of a novel death domain-containing adaptor molecule for ectodysplasin-A receptor that is mutated in crinkled mice. *Curr Biol* 2002 Mar 5; **12** (5): 409-413.
31. Cui CY, Durmowicz M, Ottolenghi C, Hashimoto T, Griggs B, Srivastava AK, *et al.* Inducible mEDA-A1 transgene mediates sebaceous gland hyperplasia and differential formation of two types of mouse hair follicles. *Hum Mol Genet* 2003 Nov 15; **12** (22): 2931-2940.
32. Mustonen T, Pispá J, Mikkola ML, Pummila M, Kangas AT, Pakkasjarvi L, *et al.* Stimulation of ectodermal organ development by Ectodysplasin-A1. *Dev Biol* 2003 Jul 1; **259** (1): 123-136.
33. Newton K, French DM, Yan M, Frantz GD, Dixit VM. Myodegeneration in EDA-A2 transgenic mice is prevented by XEDAR deficiency. *Mol Cell Biol* 2004 Feb; **24** (4): 1608-1613.
34. Tucker AS, Headon DJ, Courtney JM, Overbeek P, Sharpe PT. The activation level of the TNF family receptor, Edar, determines cusp

- number and tooth number during tooth development. *Dev Biol* 2004 Apr 1; **268** (1): 185-194.
35. Pispa J, Mustonen T, Mikkola ML, Kangas AT, Koppinen P, Lukinmaa PL, *et al.* Tooth patterning and enamel formation can be manipulated by misexpression of TNF receptor Edar. *Dev Dyn* 2004 Oct; **231** (2): 432-440.
 36. Chang SH, Jobling S, Brennan K, Headon DJ. Enhanced Edar signalling has pleiotropic effects on craniofacial and cutaneous glands. *PLoS One* 2009; **4** (10): e7591.
 37. Renner F, Schmitz ML. Autoregulatory feedback loops terminating the NF-kappaB response. *Trends Biochem Sci* 2009 Mar; **34** (3): 128-135.
 38. Skaug B, Jiang X, Chen ZJ. The role of ubiquitin in NF-kappaB regulatory pathways. *Annu Rev Biochem* 2009; **78**: 769-796.
 39. Coornaert B, Carpentier I, Beyaert R. A20: central gatekeeper in inflammation and immunity. *J Biol Chem* 2009 Mar 27; **284** (13): 8217-8221.
 40. Lee EG, Boone DL, Chai S, Libby SL, Chien M, Lodolce JP, *et al.* Failure to regulate TNF-induced NF-kappaB and cell death responses in A20-deficient mice. *Science* 2000 Sep 29; **289** (5488): 2350-2354.
 41. Boone DL, Turer EE, Lee EG, Ahmad RC, Wheeler MT, Tsui C, *et al.* The ubiquitin-modifying enzyme A20 is required for termination of Toll-like receptor responses. *Nat Immunol* 2004 Oct; **5** (10): 1052-1060.
 42. Hitotsumatsu O, Ahmad RC, Tavares R, Wang M, Philpott D, Turer EE, *et al.* The ubiquitin-editing enzyme A20 restricts nucleotide-binding

- oligomerization domain containing 2-triggered signals. *Immunity* 2008 Mar; **28** (3): 381-390.
43. Vereecke L, Beyaert R, van Loo G. The ubiquitin-editing enzyme A20 (TNFAIP3) is a central regulator of immunopathology. *Trends Immunol* 2009 Aug; **30** (8): 383-391.
44. Vereecke L, Sze M, Guire CM, Rogiers B, Chu Y, Schmidt-Supprian M, *et al.* Enterocyte-specific A20 deficiency sensitizes to tumor necrosis factor-induced toxicity and experimental colitis. *J Exp Med* Jul 5; **207** (7): 1513-1523.
45. Jonkers J, Meuwissen R, van der Gulden H, Peterse H, van der Valk M, Berns A. Synergistic tumor suppressor activity of BRCA2 and p53 in a conditional mouse model for breast cancer. *Nat Genet* 2001 Dec; **29** (4): 418-425.
46. Massoumi R, Chmielarska K, Hennecke K, Pfeifer A, Fassler R. Cyld inhibits tumor cell proliferation by blocking Bcl-3-dependent NF-kappaB signaling. *Cell* 2006 May 19; **125** (4): 665-677.
47. Ramirez A, Page A, Gandarillas A, Zanet J, Pibre S, Vidal M, *et al.* A keratin K5Cre transgenic line appropriate for tissue-specific or generalized Cre-mediated recombination. *Genesis* 2004 May; **39** (1): 52-57.
48. Zhang M, Brancaccio A, Weiner L, Missero C, Brissette JL. Ectodysplasin regulates pattern formation in the mammalian hair coat. *Genesis* 2003 Sep; **37** (1): 30-37.

49. Mou C, Thomason HA, Willan PM, Clowes C, Harris WE, Drew CF, *et al.* Enhanced ectodysplasin-A receptor (EDAR) signaling alters multiple fiber characteristics to produce the East Asian hair form. *Hum Mutat* 2008 Dec; **29** (12): 1405-1411.
50. Mauro C, Pacifico F, Lavorgna A, Mellone S, Iannetti A, Acquaviva R, *et al.* ABIN-1 binds to NEMO/IKKgamma and co-operates with A20 in inhibiting NF-kappaB. *J Biol Chem* 2006 Jul 7; **281** (27): 18482-18488.
51. Schmidt-Ullrich R, Tobin DJ, Lenhard D, Schneider P, Paus R, Scheidereit C. NF-kappaB transmits Eda A1/EdaR signalling to activate Shh and cyclin D1 expression, and controls post-initiation hair placode down growth. *Development* 2006 Mar; **133** (6): 1045-1057.
52. Tewari M, Wolf FW, Seldin MF, O'Shea KS, Dixit VM, Turka LA. Lymphoid expression and regulation of A20, an inhibitor of programmed cell death. *J Immunol* 1995 Feb 15; **154** (4): 1699-1706.
53. Scott ML, Fujita T, Liou HC, Nolan GP, Baltimore D. The p65 subunit of NF-kappa B regulates I kappa B by two distinct mechanisms. *Genes Dev* 1993 Jul; **7** (7A): 1266-1276.
54. Beg AA, Sha WC, Bronson RT, Baltimore D. Constitutive NF-kappa B activation, enhanced granulopoiesis, and neonatal lethality in I kappa B alpha-deficient mice. *Genes Dev* 1995 Nov 15; **9** (22): 2736-2746.
55. Klement JF, Rice NR, Car BD, Abbondanzo SJ, Powers GD, Bhatt PH, *et al.* IkappaBalpha deficiency results in a sustained NF-kappaB response and severe widespread dermatitis in mice. *Mol Cell Biol* 1996 May; **16** (5): 2341-2349.

56. Cui CY, Schlessinger D. EDA signaling and skin appendage development. *Cell Cycle* 2006 Nov 1; **5** (21): 2477-2483.
57. Bosanac I, Wertz IE, Pan B, Yu C, Kusam S, Lam C, *et al.* Ubiquitin binding to A20 ZnF4 is required for modulation of NF-kappaB signaling. *Mol Cell* 2010 Nov 24; **40** (4): 548-557.
58. Wertz IE, O'Rourke KM, Zhou H, Eby M, Aravind L, Seshagiri S, *et al.* De-ubiquitination and ubiquitin ligase domains of A20 downregulate NF-kappaB signalling. *Nature* 2004 Aug 5; **430** (7000): 694-699.
59. Mustonen T, Ilmonen M, Pummila M, Kangas AT, Laurikkala J, Jaatinen R, *et al.* Ectodysplasin A1 promotes placodal cell fate during early morphogenesis of ectodermal appendages. *Development* 2004 Oct; **131** (20): 4907-4919.
60. Pummila M, Fliniaux I, Jaatinen R, James MJ, Laurikkala J, Schneider P, *et al.* Ectodysplasin has a dual role in ectodermal organogenesis: inhibition of Bmp activity and induction of Shh expression. *Development* 2007 Jan; **134** (1): 117-125.
61. Fliniaux I, Mikkola ML, Lefebvre S, Thesleff I. Identification of dkk4 as a target of Eda-A1/Edar pathway reveals an unexpected role of ectodysplasin as inhibitor of Wnt signalling in ectodermal placodes. *Dev Biol* 2008 Aug 1; **320** (1): 60-71.
62. Gaide O, Schneider P. Permanent correction of an inherited ectodermal dysplasia with recombinant EDA. *Nat Med* 2003 May; **9** (5): 614-618.

Acknowledgements

We thank Dr. A. Bredan for editing the manuscript. We are grateful to Dr. Jos Jonkers for sharing the K14-Cre transgenic mice, to Dr. Pascal Schneider for donating recombinant Fc-EDA-A1, and to Ingrid Fliniaux for technical help. We thank Ingo Haase for helpful discussions and suggestions. We are grateful to Dimitri Huyghebaert, Laetitia Bellen and Carine Van Laere for animal care. S.L. and G.v.L. are postdoctoral researchers with the “Fonds voor Wetenschappelijk Onderzoek-Vlaanderen” (FWO). L.V. and K.V. are PhD fellows with the “Instituut voor Innovatie door Wetenschap en Technologie” (IWT), C.M. is a PhD fellow with the FWO and S.Le. was supported by the Marie Curie Early Stage Training program (FP6) and the Finnish Cultural Foundation. This research has been supported by the Flanders Institute for Biotechnology (VIB), Ghent University and several grants: FWO Odysseus Grant (to G.v.L.), FP6 Integrated Project Epistem LSHB-CT-2005-019067, COST action SKINBAD BM0903, FP6 ApopTrain, MRTN-CT-035624; FP7 EC RTD Integrated Project, Apo-Sys, FP7-200767, “Interuniversity Attraction Poles program” (IAP6/18), “Belgian Foundation against Cancer”, FWO (3G.0218.06, G.0089.10, G.0619.10), “Strategic Basis Research program” of the IWT, “Centrum voor Gezwellziekten”, “Concerted Research Actions” (GOA) and “Group-ID Multidisciplinary Research Platform” programs of Ghent University, and Academy of Finland and Sigrid Jusélius Foundation grants (to M.L.M.). P.V. holds a Methusalem grant (BOF09/01M00709) from the Flemish Government.

Figure Legends

Figure 1. Generation of A20^{EKO} mice. (A) Photograph of A20^{EKO} mouse and A20^{FL/FL} control mouse. (B) Southern blot analysis of DNA from epidermis and dermis from A20^{EKO} mice, and DNA from isolated keratinocytes of WT and A20^{EKO} mice. (C) Protein extracts from epidermal tissue, derived from keratinocyte (A20^{EKO})-specific knockouts, were analyzed by western blotting with an A20-specific antibody. The A20 protein band is indicated with an arrowhead, * indicates aspecific bands.

Figure 2. A20^{EKO} display mild keratinocyte hyperproliferation. (A) Sections of back skin of A20^{FL/FL} and A20^{EKO} mice were stained with hematoxylin and eosin and analyzed by light microscopy (scale bar: 100 μ m). (B) Ki-67-positive staining (dark brown nuclei) of back skin sections from A20^{FL/FL} and A20^{EKO} mice (scale bar: 100 μ m). (C) Quantification of the percentage of Ki-67-positive basal layer keratinocytes in sections of back skin of A20^{FL/FL} and A20^{EKO} mice.

Figure 3. A20^{EKO} mice have thinner hair with defective cuticle. (A) Picture of the coat hairs of A20^{FL/FL} and A20^{EKO} mice. (B) Hair from the back of A20^{FL/FL} and A20^{EKO} mice was epilated. Microscopic examination shows the presence of guard hair, awl hair, zigzag hair and auchene hair in A20^{FL/FL} control mice. A20^{EKO} mice have only straight or curly hair. ah = awl hair, au = auchene hair, gh = guard hair, zz = zigzag hair. (C,D) SEM picture of hair from A20^{FL/FL} and A20^{EKO} mice (scale bar: 10 μ m). (E,F) TEM of sections through back skin of A20^{FL/FL} and A20^{EKO} mice showing detail of a section through a hair follicle

(scale bar: 500 nm). The A20^{EKO} mice have a hyperplastic and disorganized cuticular layer. h= hair shaft, c = cuticular layer.

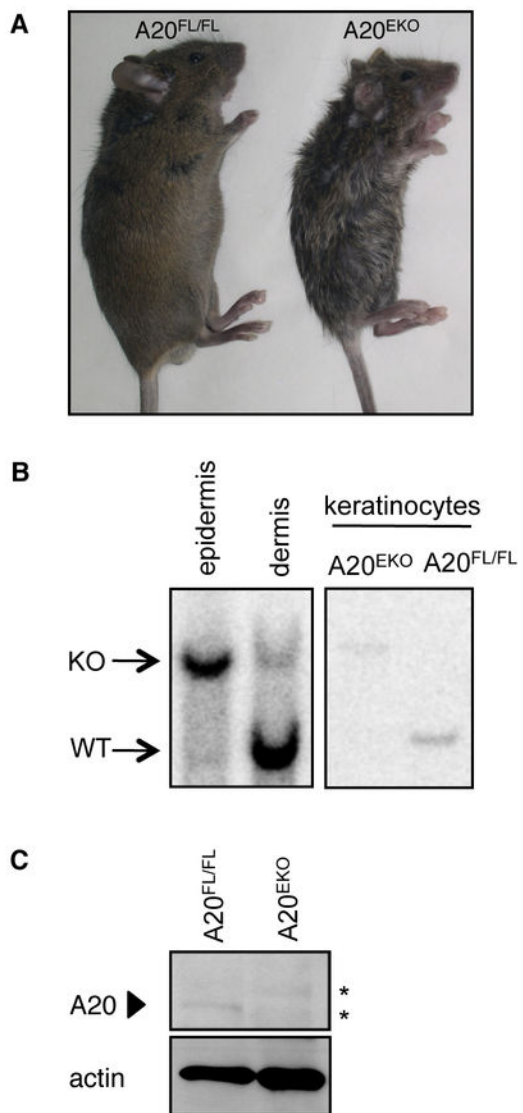
Figure 4. Additional hallmarks of the A20^{EKO} phenotype that phenocopy the EDA transgenes. (A) Picture of paws viewed with a binocular microscope shows that A20^{EKO} mice have longer nails than control littermates. (B) Macroscopic analysis of the tails shows more curly tail hairs and larger scale-like folds on A20^{EKO} mice. (C) Sebocytes in skin sections from A20^{EKO} and control mice were stained with an anti-adipophilin antibody. (scale bar: 500 μ m) (D) The surface areas of the sections through the sebaceous gland were determined based on this staining using Volocity image analysis software, and the mean surface areas in A20^{EKO} and control mice were compared.

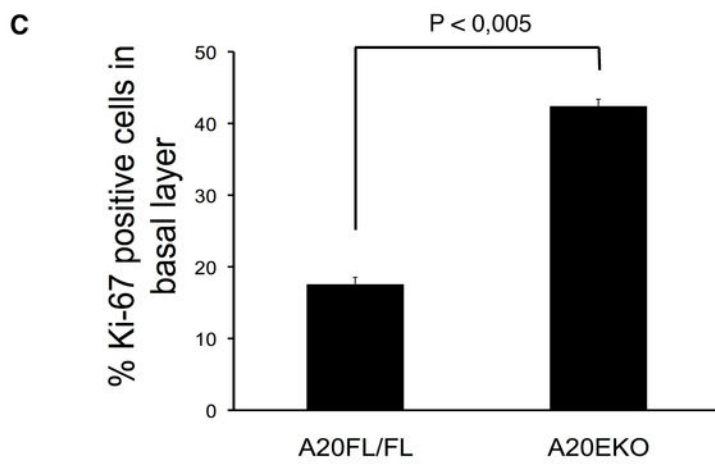
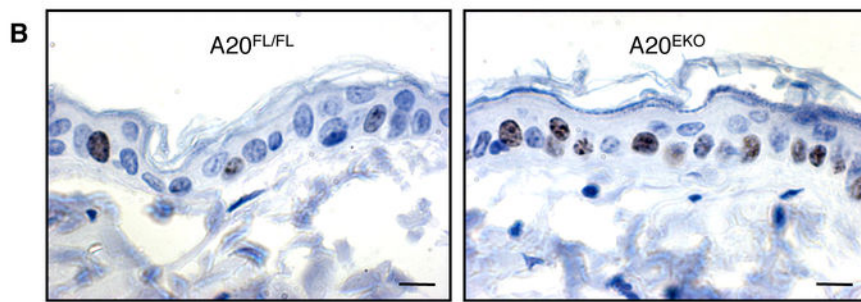
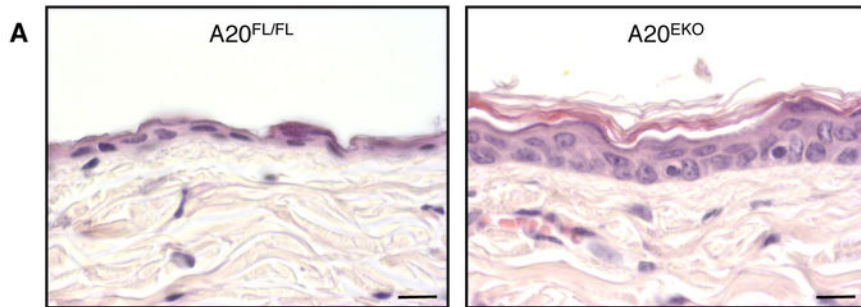
Figure 5. EDA-A1 induces A20 as a negative regulator of EDAR-induced NF- κ B activation. (A) Measurement of NF- κ B luciferase activity in lysates of HEK293T cells transfected with combinations of an NF- κ B-dependent luciferase reporter plasmid and plasmids encoding A20, IKK2 or EDAR. Cells were stimulated with 10,000 U/ml TNF for 4 h. (B) Inhibition of EDAR-induced NF- κ B luciferase activity, by different A20 domains. A20-N: DUB domain of A20, A20-C: C-terminal Zn-finger domains. (C) Inhibition of EDAR induced NF- κ B luciferase activity by an A20 DUB mutant (A20 D100A/C103A). (D) A20 expression levels were determined by quantitative PCR analysis of E14 EDA^{-/-} skin explants treated with Fc-EDA-A1 for 2 or 4 h. Error bars indicate S.D. ***, $p < 0,001$. (E) Skin explants were put in hanging drops and left

untreated or treated with 250 ng/mL Fc-EDA-A1 for 6 hours. Protein extracts were analyzed for A20 expression by western blot.

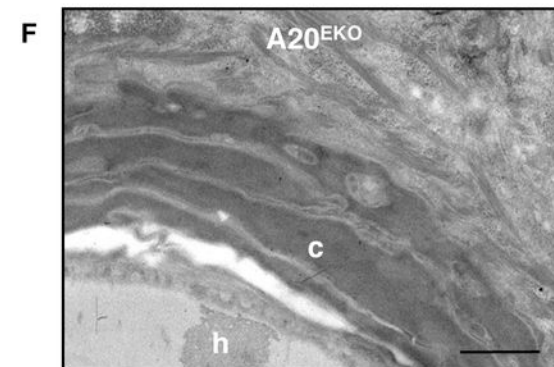
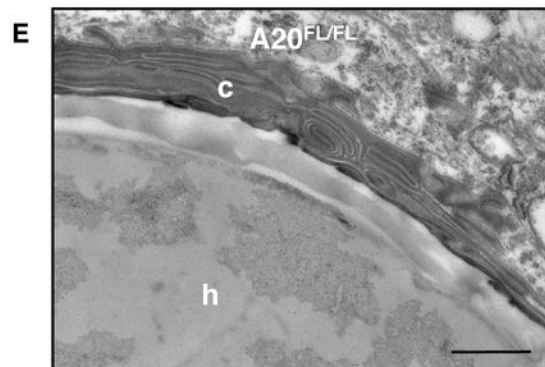
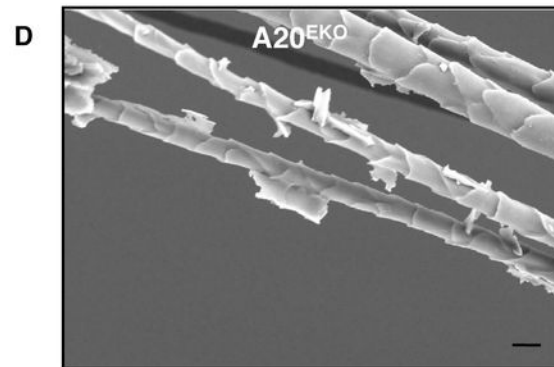
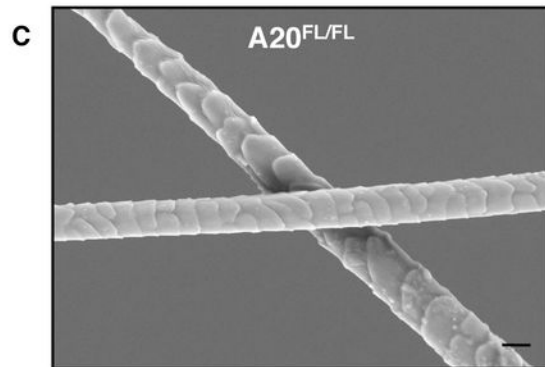
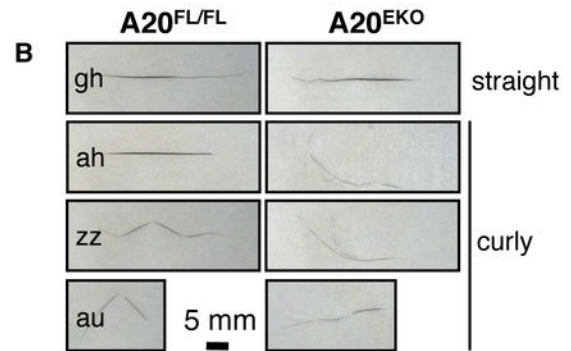
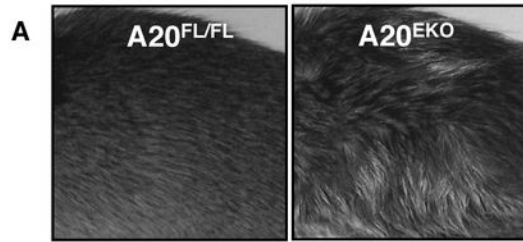
Figure 6. EDA-A1 stimulation induces A20 expression in developing hair placodes. (A) Expression of A20 was visualized by whole mount *in situ* hybridization on EDA-deficient and WT E14 embryos, dark bluish color indicates a positive *in situ* signal. The right panel depicts a vibratome section through a hair placode (arrow). (B) Whole mount *in situ* hybridization was performed on E12 embryos using an anti-sense probe for A20 (left panels) or Wnt10b (right panels) as a positive control for expression in the tooth placode (upper panels) and mammary bud (lower panels). F= forelimb; H= hindlimb; I= incisor placode; m= mammary bud; M= molar placode; T= tongue.

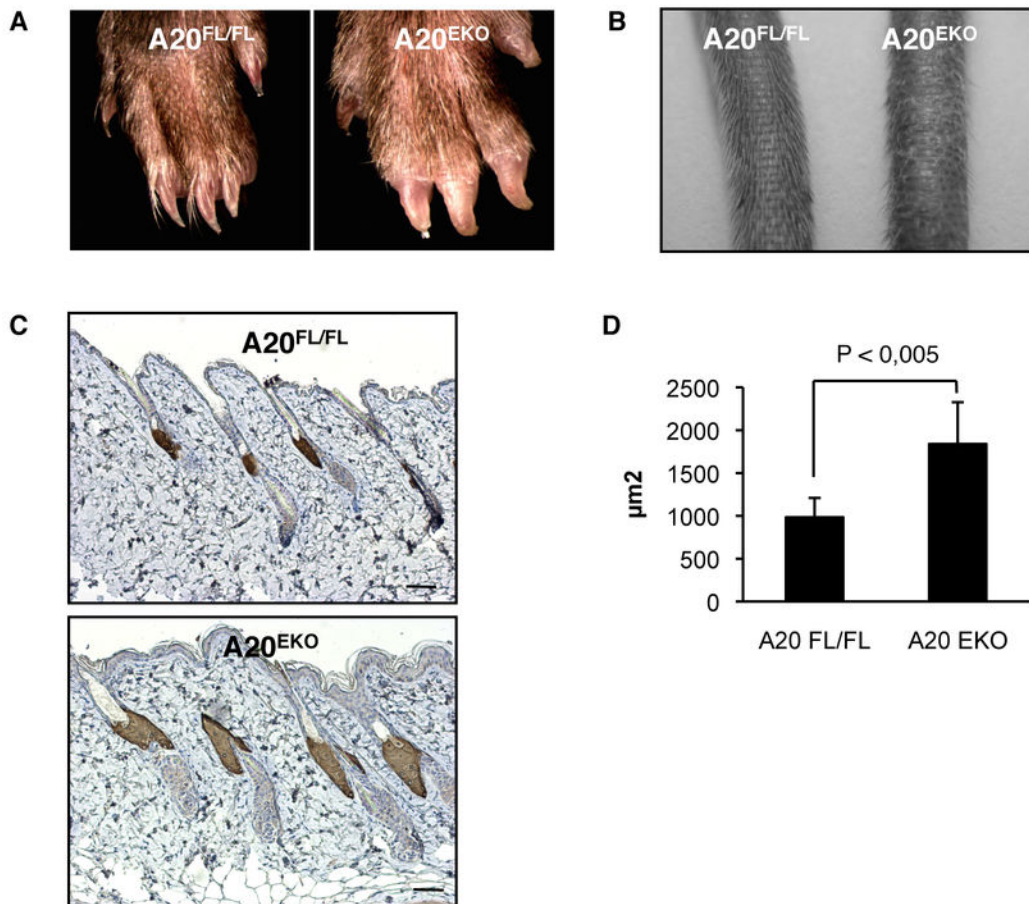
Supplementary Figure 1. (A) Expression analysis of different E-tagged A20 deletion mutants from the experiment shown in Fig. 5B. (B) Expression analysis of E-tagged A20 point mutant from the experiment shown in Fig. 5C.

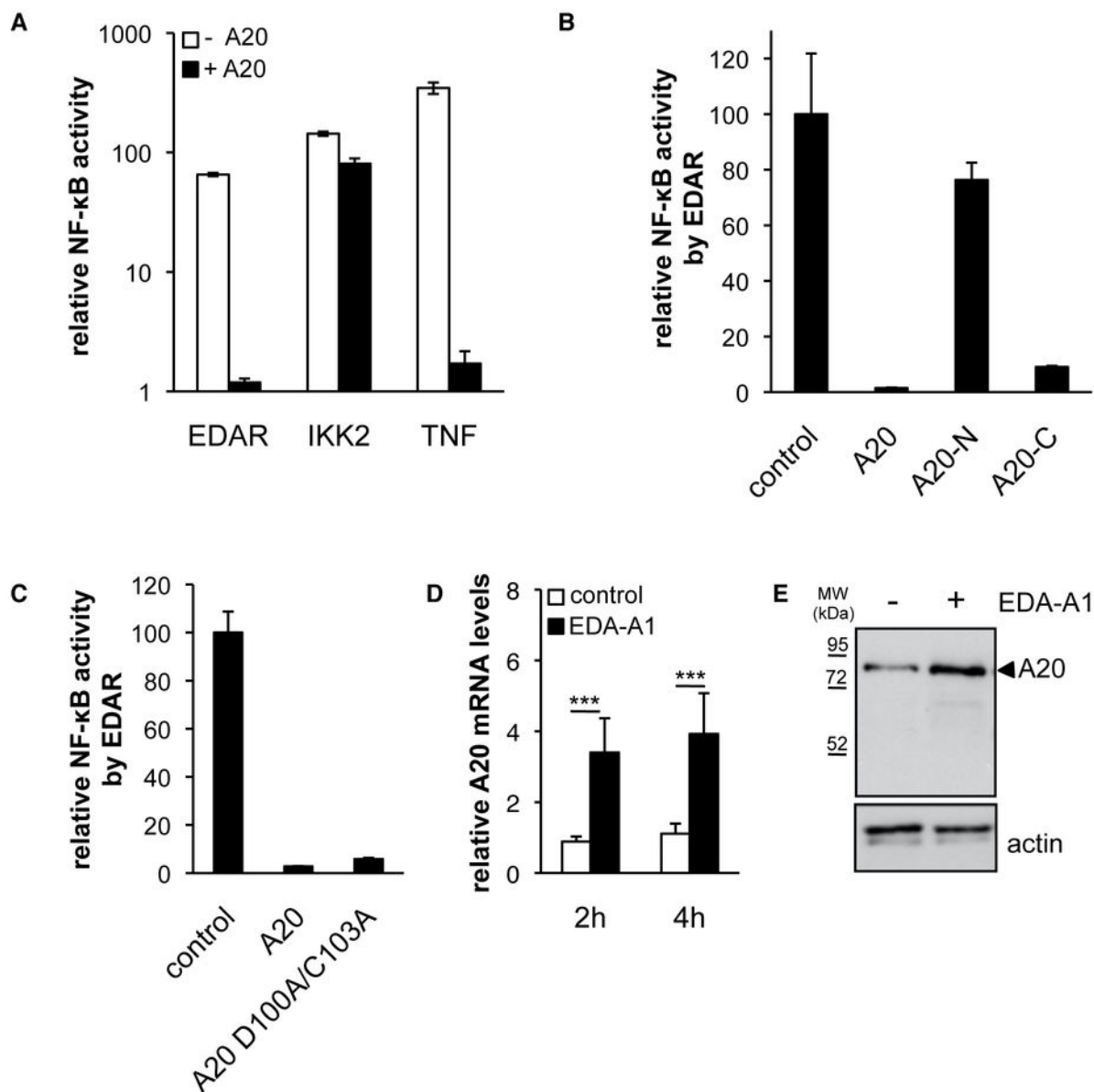




Lippens_Fig3







Lippens_Fig6

